Gondwana Research 21 (2012) 624–636

Contents lists available at ScienceDirect

Gondwana Research

journal homepage: www.elsevier.com/locate/gr

Tectono-sequence stratigraphy and U–Pb zircon ages of the Rincón Blanco Depocenter, northern Cuyo Rift, Argentina

Silvia Barredo [a], Farid Chemale [b], Claudia Marsicano [c], Janaína N. Ávila [d], Eduardo G. Ottone [c], Victor A. Ramos [a,c,*]

[a] Laboratorio de Tectónica Andina, Departamento de Ciencias Geológicas, Facultad de Ciencias Exactas y Naturales, Universidad de Buenos Aires, Argentina
[b] Núcleo de Geologia, Universidade Federal de Sergipe, Brazil
[c] CONICET- Departamento de Ciencias Geológicas, Facultad de Ciencias Exactas y Naturales, Universidad de Buenos Aires, Argentina
[d] Research School of Earth Sciences, Australian National University, Australia

ARTICLE INFO

Article history:
Received 21 August 2010
Received in revised form 11 May 2011
Accepted 29 May 2011
Available online 12 June 2011

Handling Editor: E. Tohver

Keywords:
Triassic rifting
U–Pb in situ geochronology
Tectono-sequences
South America

ABSTRACT

Extensional processes that followed the Gondwanan Orogeny rise to the development of a series of rift basins along the continental margin over older accreted Eopaleozoic terranes. Stratigraphic, structural, paleontological, and isotopic studies are presented in this work in order to constrain the ages of the sedimentary infilling and to analyze the tectosedimentary evolution of one of the Cuyo basin depocenters, known as Rincón Blanco. This asymmetrical half-graben was filled by continental sediments under a strong tectonic control. The infilling was strongly controlled by tectonics which in term produced distinctive features along the whole sedimentary sequence. Using a combination of lithological and structural data the infilling was subdivided into packages of genetically linked units bounded by regional extended surfaces. Several tuffs and acid volcanic rocks have been collected across the whole section of the Rincon Blanco sub-basin for SHRIMP and LA-MC-ICPMS U–Pb zircon dating. The ages obtained range from 246.4 ± 1.1 Ma to 230.3 ± 1.5 Ma which is the time elapsed for the deposition of three tectono-sequence units separated by regional unconformities and mainly constrained to the Middle Triassic. They are interpreted as a result of a reactivation of the extensional system that has evolved along strike as segments of faults that linked together and/or as laterally propagating faults. Regional correlation with coeval rift basins permits to establish north-south propagation in the extensional regime along the western margin of SW Gondwana. This trending started in the lowermost Triassic and extended until the latest Triassic. Two of them were precisely correlated with Cerro Puntudo and Cacheuta half-graben systems. The new data indicate that the three sequences were mostly deposited during the Middle Triassic (246 to 230 Ma), with no evidence of sedimentation during Norian and Rhaetian, which is in conflict with some previous biostratigraphic studies.

1. Introduction

The Gondwanian Orogeny affected the western margin of southern South America during the Mississippian to the Early Triassic as part of the final amalgamation of the Pangea (see Gregori et al., 2008; and Ramos, 2008, for contrasting scenarios). Soon after the formation of this supercontinent, a series of elongated NW-trending rifts (e.g. Bermejo, Marayes and Cuyo) was developed in this margin related to the Pangea breakup during Triassic–Early Jurassic times (Fig. 1) (Uliana et al., 1989; Ramos and Kay, 1991; Brito Neves et al., 2002; Veevers, 2005, among others). The inception of these rifts was controlled by previous NW-trending Paleozoic sutures related to the late Paleozoic orogenies, and the extension was concentrated in the hanging-wall of these old weakness zones (Mpodozis and Ramos, 2008; Ramos, 2009). The rift basins were filled mainly with continental clastic and pyroclastic sediments. Among them, the Cuyo Basin, one of the important oil producing basins of the central western region of Argentina, corresponds to a passive rift developed during differential intraplate stresses (Strelkov and Alvarez, 1984; Kokogian et al., 1993, 2001). It is composed of several asymmetric half-grabens linked by accommodation zones (Legarreta et al., 1992; Barredo, 2005). This geometry and the coeval tectonic activity are thought to be one of the major factors in controlling the evolution of the sedimentary sequences which gave place to complex environmental relationships. This pattern results in an intricate stratigraphy, which has been partly, solved using the well-preserved plant record of these successions (Stipanicic, 1979, 2002; Spalletti et al., 1999). However, the lack of an

* Corresponding author at: Laboratorio de Tectónica Andina, Departamento de Ciencias Geológicas, Facultad de Ciencias Exactas y Naturales, Universidad de Buenos Aires, Argentina.
E-mail addresses: silvia@gl.fcen.uba.ar (S. Barredo), farid.chemale@ufs.br (F. Chemale), claumar@gl.fcen.uba.ar (C. Marsicano), janaina.avila@anu.edu.au (J.N. Ávila), ottone@gl.fcen.uba.ar (E.G. Ottone), andes@gl.fcen.uba.ar (V.A. Ramos).

1342-937X/$ – see front matter © 2011 International Association for Gondwana Research. Published by Elsevier B.V. All rights reserved.
doi:10.1016/j.gr.2011.05.016

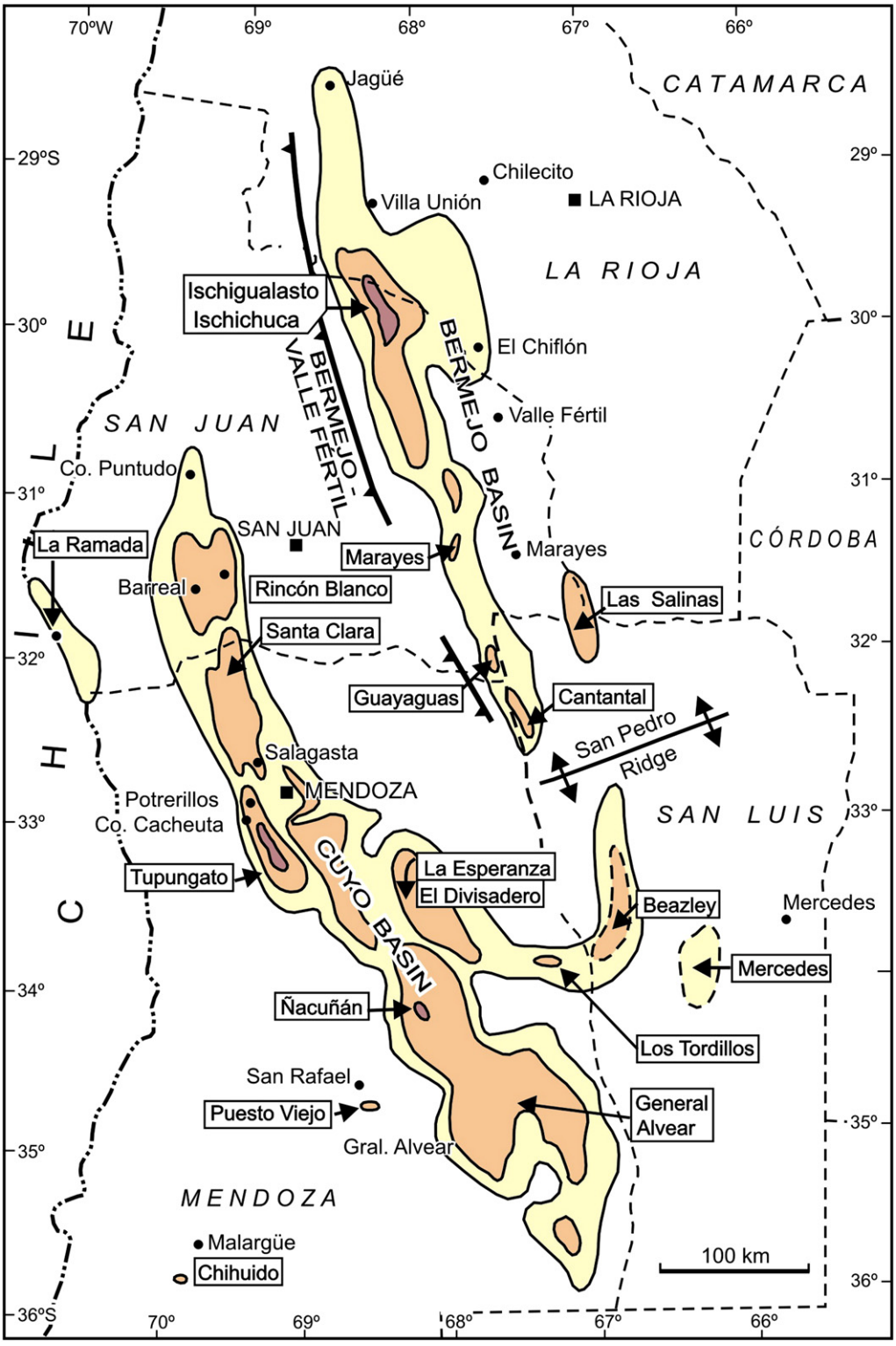

Fig. 1. Triassic rift basins in central Argentina with location of the study area of Rincón Blanco, Cacheuta and other related sub-basins of the large Cuyo Basin (modified from Stipanicic, 2002; Mpodozis and Ramos, 2008).

absolute dating framework and the subsequent structural complexities caused by compressional Andean deformation has meant that stratigraphic analysis still has a large margin of uncertainty. However, Avila et al. (2003, 2006) and Spalletti et al. (2008) published the first U–Pb SHIRMP ages for the Río Mendoza and Potrerillos formations of the Cacheuta depocenter, respectively, establishing two potential chronostratigraphic horizons for stratigraphic correlations. More recently, a third U–Pb SHIRMP age for the northernmost outcrops of the basin (Cerro Puntudo Formation) has provided a further chronocorrelation line for several depocenters of the basin (Mancuso et al., 2010).

In the Rincón Blanco sub-basin, one of the northernmost sections of the Cuyo Basin (López Gamundí, 1994), located in the San Juan province, the non-marine Triassic infilling has been studied in detail using its

floral content and lithostratigraphy (Borrello and Cuerda, 1965; Yrigoyen and Stover, 1969; Stipanicic, 1979, 2002; Barredo and Stipanicic, 2002). Additionally, sequence stratigraphy has also been applied in an attempt to establish a more precise correlation between the active and flexural margins (Spalletti, 1999; Barredo, 2004) but some uncertainties remained because of the lack of absolute age control in the depocenter as a whole.

The objective of this work is to establish the timing of deposition of the different tectono-sequences in the Rincón Blanco sub-basin as a whole and to provide new chronostratigraphic horizons for more accurate correlation between this depocenter, the Cacheuta sub-basin and the Puntudo halfgraben (Fig. 1), located south and north respectively. Detailed stratigraphic and structural field mapping at scale a 1:15,000 scale combined with in situ U–Pb dating (SHRIMP and LA-MC-ICPMS) are employed herein. Furthermore it is attempted here to analyze the tectonic evolution of this rift integrating the precise ages obtained with the sedimentary, structural, and paleontological data. Finally, the timing of this rift scheme will be integrated to the others coeval extensional basins in other to refine the tectonic framework of the Pangea break-up along the South American margin during Triassic times.

2. Geological setting

The Triassic Rincón Blanco sub-basin is an elongate trough located in the Precordillera fold and thrust belt at 31°24′–31° 33′ south (Fig. 2). It is 5 km wide and stretches approximately 25 km N–S. The infill consists of almost 3000 m of non-marine Triassic coarse conglomerates interfingered with sandstones, shales, tuffs, tuffaceous mudstones and bimodal volcanic rocks composed of rhyolites and rhyolitic tuffs associated with the Choiyoi volcanic rocks. Alkaline basalts are also present but only on the flexural margin of the basin outside of the study area.

At present, it is a tight asymmetric syncline bounded on the west by Palaeozoic rocks thrust up east-verging typical Andean thrusts which isolated the flexural margin from the active margin (see Fig. 2). Additionally, west-verging backthrusts truncate the southern and eastern sector of the basin leading to complex field relationships between the Triassic units (Barredo, 2004). Only the southernmost portion of the master fault is outcropping because it is truncated by the Tontal East Fault, as part of a backthrust system (Fig. 2). It is a north striking down-to-the west normal fault which dips at 70° at the present–day erosion level, but at depth it is assumed to be listric. Using the architecture and features of the sedimentary record it was established that it was composed of at least two propagating segments separated by transfer zones which were probably connected during sag phases (Barredo, 2004).

The basement of the Triassic sedimentary rocks in the central and southern part is formed by tightly folded marine deposits of Ordovician age. In the north, outside of the study area, the base of the Triassic sequences is formed by the Del Salto Formation, a marine to continental unit which contains Cisuralian brachiopods (Manceñido, 1973). The upper part of the section is formed by coarse conglomerates interbedded with some andesites and tuffs. This upper member has been recently assigned to the Triassic (Barredo and Stipanicic, 2002).

The infilling of the basin is represented by the Rincón Blanco Group and the Marachemill facies (Barredo, 2004). The Rincón Blanco Group is composed of, from base to top: the Ciénaga Redonda, Cerro Amarillo, Panul, Corral de Piedra, Carrizalito, and Casa de Piedra formations.

The Ciénaga Redonda and Cerro Amarillo Formations (Fig. 3) are characterized by three facies association, alluvial fans, ephemeral streams, and lacustrine deposits related to the first stage of rifting when the basin constituted a simple fault-bounded basin. Along-strike variations in fault displacement are responsible for variations in the thickness and geometry of these syn-extensional units. They are thickest to the center of the border fault, near the Amarillo and Bola hills (Fig. 2), nearly reaching 1200 m, and thin toward the north, to the tip of the fault where they are almost 100 meters thick; this pinch-out is also observed to the west. The 400 m thick Ciénaga Redonda Formation unconformably overlies Ordovician rocks. It is composed of conglomerates and breccias interpreted as cohesive debris flow fan deposits and uncohesive debris flows developed in non-canalized sheet flows. Interfingered with these facies are ignimbrites and scarce rhyolitic and lithic tuffs. This facies association is related to proximal alluvial fans and alluvial fans braidplain settings dominated by ephemeral streams.

The Cerro Amarillo Formation is characterized by laterally discontinuous sheet-like beds of massive and horizontally bedded sandstones stacked in packages of few meters thick with alternations of conglomerates. This sequence corresponds to short-lived, wide, poorly canalized flows or low energy sheet flows in ephemeral streams of fans and bajadas. More distally, there are silty-sandstones, massive to parallel-laminated mudstones with desiccation cracks and anhydrite lenses alternating with black (lignitic?) shales. This facies association corresponds to a shallow lacustrine environment. Near the top of the formation, there are lenticular, well-sorted sandstones, and mudstones with interbedded conglomerates. Individual sandstone beds show erosional bases; they are normally graded, massive or trough to planar-cross stratified with lag veneers. These beds grade to fine sandstones with ripple-cross lamination and finely laminated shales which interfinger with tuffaceous sandstones and scarce tuffs. These facies correspond to deposits of braided fluvial systems with a predominantly axial paleoflow.

Chronostratigraphic correlation is uncertain because the Ciénaga Redonda and Cerro Amarillo Formations represent a restricted stratigraphic wedge. The scarce fossil record represented by woody plant remains and scarce, poorly preserved miospores (Barredo et al., 1999) makes it difficult to correlate these two units with those identified on the flexural margin. This part of the succession was considered upper Middle Triassic in age by Stipanicic (1972) on the basis of stratigraphic relationships.

The Panul Formation overlies these units and is separated from them by a regional unconformity of approximately 5°. It has been interpreted as the result of a new extensional period (or rift II) by Barredo (2004). It is composed of amalgamated conglomerates with angular-basement derived lithologies and sandstones and rhyolites from the underlying Triassic units. This sequence passes upwards to lenticular bodies of conglomerates and pebbly sandstones with erosive bases. Internally they are massive or with trough-cross stratification and are normally graded. They correspond to alluvial fan and braided fluvial facies association. The volcaniclastic content is extremely high compared with the underlying units and consists of tuffs, and tuffaceous sandstones and conglomerates.

The Corral de Piedra Formation is comprised of fining–upward tabular sequences consisting of fine conglomerates and sandstones with trough-cross bedding, lag deposits, and erosive bases. They grade into medium fine-grained, moderately to well sorted tabular sandstones/tuffaceous sandstones, reworked tuffs, with thick overbank mudstones at top. These characteristics and the occurrence of lateral accretion surfaces indicate that this facies was deposited by meandering fluvial systems. This unit was previously considered Middle to Late Triassic in age on the basis of its floral fossil content with elements of the “Ipswich Microflora” and scarce plant remains that mostly include peltasperms (*Lepidopteris madagascariensis* Carpentier and Antevsia sp.) and Bennettitales (*Taeniopteris* sp.) together with probable Coniferales and pteridosperm fronds (Barredo y Stipanicic, 2002; Ottone and Rodríguez Amenábar, 2001; Ottone, 2006; Zavattieri and Batten, 1996). Vertebrates are only represented in this unit by a quite diverse association of tetrapod tracks and trackways. They were assigned to crurotarsal archosaurs, dinosaurs, and therapsids, as representing a Late Triassic association similar to others described from equivalent levels from Gondwana (Marsicano and Barredo, 2004).

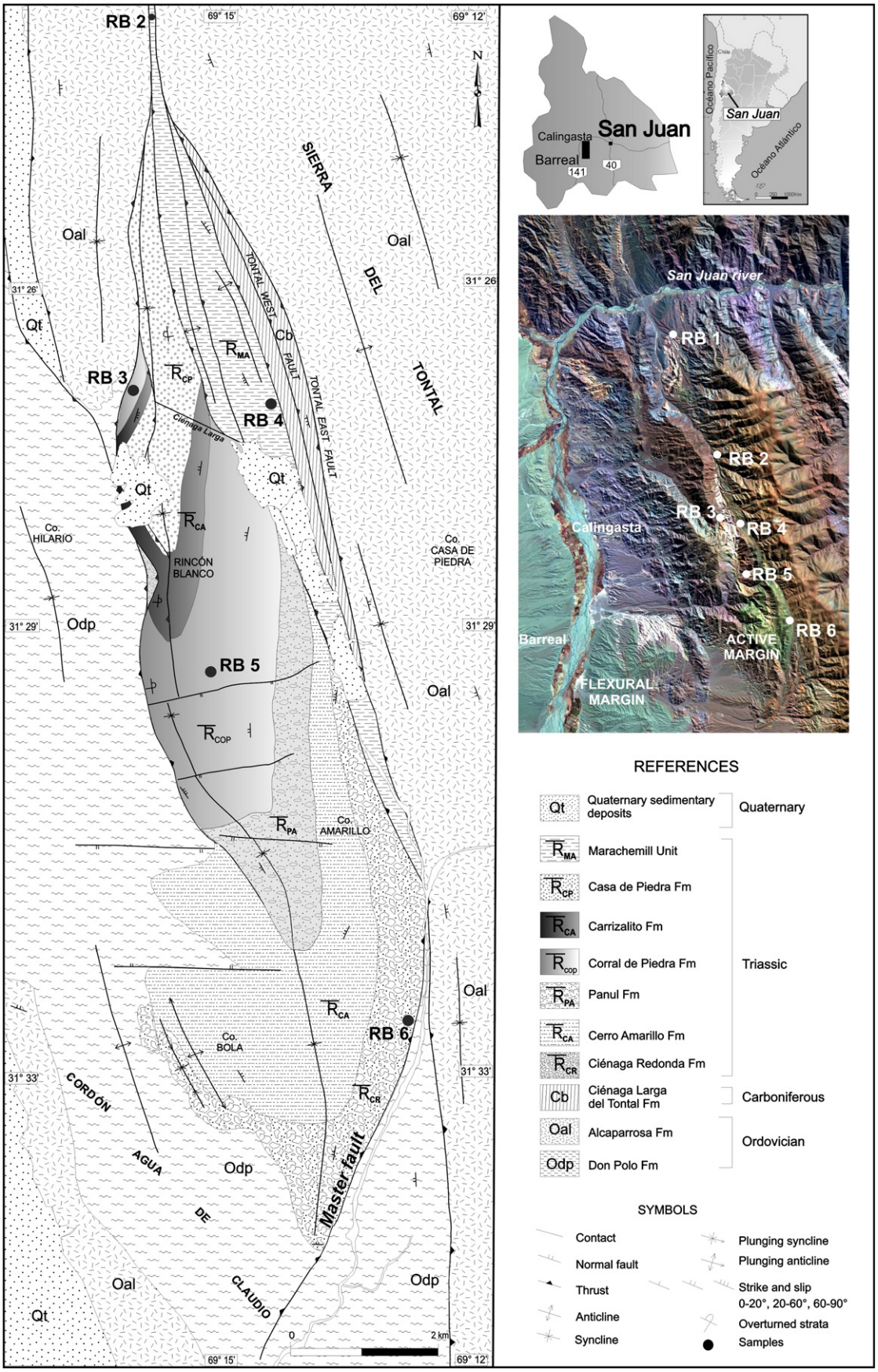

Fig. 2. Simplified geological map of the northern portion of the Cuyo Basin in the Rincón Blanco sub-basin with sample location (after Barredo, 2004).

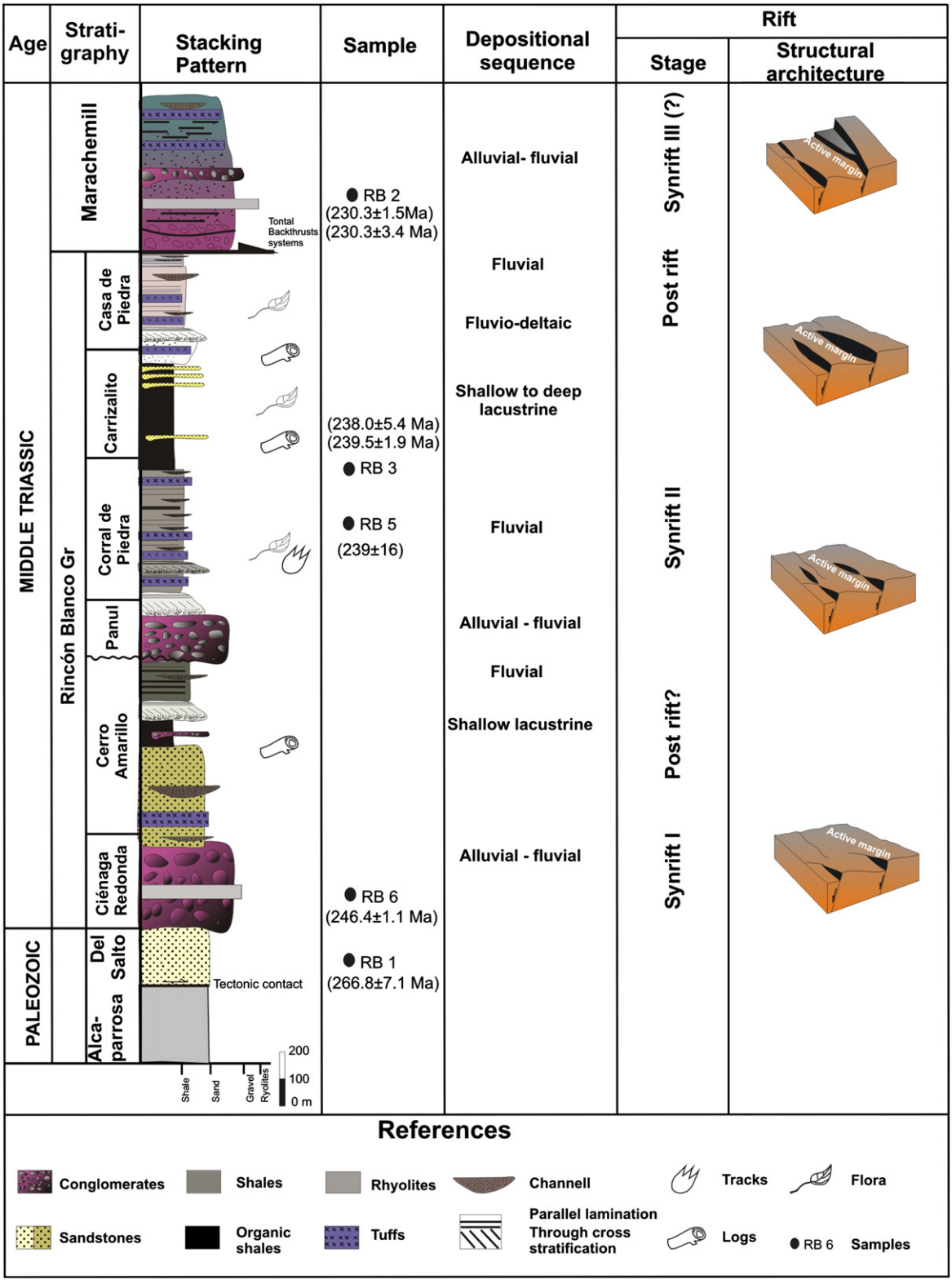

Fig. 3. Stratigraphic chart of the active margin of the Rincón Blanco halfgraben with the depositional environments and the rifting stage interpreted on the basis of the field studies and dating presented here. U–Pb zircon ages are indicated (location in Fig. 2). Additionally, a brief structural architecture is depicted.

The whole sequence vertically and laterally passes into the lacustrine facies of the Carrizalito Formation which is composed of thick massive mudstones/tuffaceous siltstones with volcaniclastic, mostly chonitic, levels. These are overlain by stratified silty sandstones and massive mudstones related to a deeper facies. Occasionally, they are associated with massive or horizontally laminated marls (30 cm in thickness) and pale-grey organic levels which consist of laminated bituminous shales with micritic calcite. Organic analysis indicates that they are oil-prone coals probably resulted from the accumulation of plant debris followed by an important bacterial decomposition event. It bears a similar palynological association to the Corral de Piedra Formation thus it was previously assigned a probable Carnian–Norian age.

In the uppermost section of this sequence, deep facies are replaced by clast-supported planar to trough-cross bedded lenticular conglomerates and sandstones interbedded with laminated mudstones and limestones interpreted as mouth bars deposits. These facies correspond to the basal levels of the Casa de Piedra Formation and are followed up section by lenticular conglomerates and sandstones with trough-cross bedding and erosive bases. They grade into fine-grained, sandstones/tuffaceous sandstones, and thick overbank mudstones which at the top interfinger with ash fall tuffs. These facies represent the initiation of fluvial systems with northwest, west and northeast paleoflows. The Casa de Piedra vegetal remains are characteristic of the Dicroidium flora. The fossil plant assemblage is relatively abundant and includes Corystospermales, (*Dicroidium incisum* (Du Toit) Anderson and Anderson, *D. odontopteroides* var. *moltense* Retallack, *D. odontopteroides* var. *obtusifolium* Johnston, *D. odontopteroides* var. *remotum* (Szajnocha) Retallack, *Xylopteris densifolia* (Du Toit) Frenguelli, *X. remotipinnulia* (Anderson and Anderson) Ottone, *X. rigida* (Dun) Jain and Delevoyras, *X. spinifolia* (Tenison-Woods) Frenguelli and *Zuberia zuberi* (Szajnocha) Frenguelli, but also *Sphenophyta* (*Neocalamites* sp.) and Cycadales (*Pseudoctenis* sp. A and P. sp. B). The palynoflora comprises miospores characteristic of the Ipswich Microflora, amorphous organic matter and the green algae *Botryococcus* (Ottone and Rodríguez Amenábar, 2001; Rodríguez Amenábar and Ottone, 2003; Ottone, 2006). The transitional character of this unit with respect to the Carrizalito Formation suggests a Late Triassic age for the Casa de Piedra Formation (Barredo and Stipanicic, 2002).

Finally, to the north-east margin of the basin a series of almost 900 m of mainly volcaniclastic and clastic rocks were interpreted as lateral facies of the Rincón Blanco Group by Borrello and Cuerda (1965) and Yrigoyen and Stover (1969). Most recently, Barredo (2004) undertook a detailed regional study of this sequence and proposed that there is not a direct correlation between these rocks and the Rincon Blanco Group and renamed them as the Marachemill Unit. The Marachemill Unit is in tectonic contact with the Rincón Blanco Group (Fig. 4). Three facies associations characterize this unit: proximal to distal alluvial fans, ephemeral streams and fluvial systems. They are characterized by thick massive, mud-rich matrix-supported red conglomerates and breccias composed of volcaniclastic and sedimentary clasts mostly associated with the underlying Rincón Blanco Group. They are interpreted as alluvial fan environments. These facies interfinger with several ignimbrites and rhyolitic tuffs levels, tuffs and tuffaceous sandstones which contrast with the Rincón Blanco Group deposits. Upwards, there are coarse massive to horizontal laminated sandstones with erosive to sharp bases, shale intraclasts and high energy structures. Laterally they are associated with flood plain deposits mostly represented by fine sandstones and shales with oxidized organic matter and desiccation cracks. These facies are interpreted as poorly canalized flows and sheet floods developed in ephemeral environments. Volcaniclastic deposits are abundant and correspond to ash fall tuffs and pyroclastic flows. Lenticular conglomerates to granular sandstones in frequently amalgamated bodies follow up section. The conglomerates are poorly sorted with sub-angular to sub-rounded clasts from the Ordovician basement, sometimes rather imbricated, and commonly resting on a scoured surface. There are also tabular beds of poorly sorted and pebbly conglomerates, dominated by scour and fill structures with massive fills and lag deposits. Overlying beds correspond to tabular sandstones with planar cross stratification with scattered pebbles at the base which grades to fine to medium sandstones with small-scale trough-cross stratification and ripple-cross lamination capped by thin beds of massive or rippled greenish grey siltstones, tuffs, and mudstones with invertebrate burrows and mudcracks. They are interpreted as having been deposited by braided fluvial systems with dominant paleocurrents to the east-northeast. Finally, mostly sandy braided stream deposits with alluvial plains are developed. Ash-fall deposits are abundant constituting thick tabular massive, sometimes laminated, deposits and reworked levels that can be interpreted as tuffaceous plains with isolated poorly developed fluvial channels.

In contrast with the inferred humid climate that governed the deposition of the uppermost Carrizalito and Casa de Piedra formations of the Rincón Blanco Group, the sedimentary environments of the Marachemil Unit evolved under marked semiarid conditions. Consequently, the fossil record is extremely different. While the Marachemill beds only recorded very scattered trace fossils and miospores, the Carrizalito and Casa de Piedra beds bear a rich flora and evidence of a diverse tetrapod association. This association enables this unit to be

Table 1
Laser operating conditions.

Laser type New Wave UP213	MC-ICP-MS Neptune
• Laser output power 6 J/cm^2 • Shot repetition rate 10 Hz • Laser spot 25 and 40 μm	• Cup configuration: Faradays ^{206}Pb, ^{208}Pb, ^{232}Th, ^{238}U MIC's ^{202}Hg, ^{204}Hg + ^{204}Pb, ^{20}7Pb • Gas input: Coolant flow (Ar) 15 l/min Auxiliary flow (Ar) 0.8 l/min Carrier flow 0.75 l/min (Ar) + 0.45 l/min (He) • Acquisition 50 cycles of 1.048 s

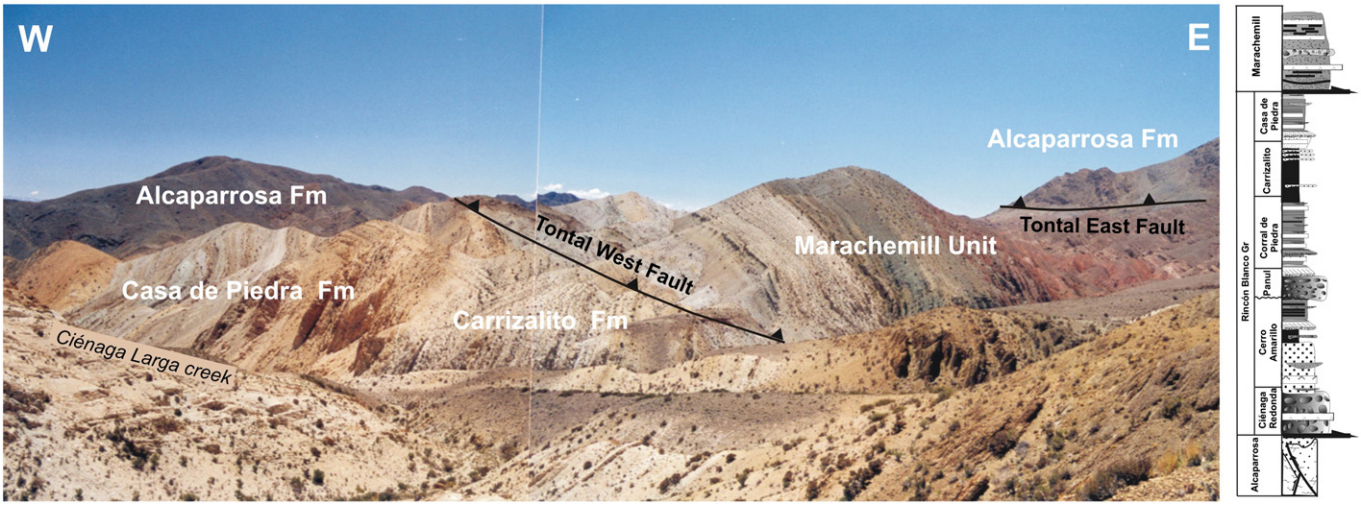

Fig. 4. The tectonic relationship between the Rincón Blanco Group and the Marachemill Unit. See the close lithological resemblance which previously had driven to consider them as a simple lateral extension of the Rincón Blanco Group.

Table 2
Summary of SHRIMP U–Pb zircon data for Rincon Blanco Subbasin samples.

GrainSpot	% $^{206}Pb_c$(2)	ppm U	ppm Th	$^{232}Th/^{238}U$	ppm $^{206}Pb^*$	$^{238}U/^{206}Pb^*$	% err	$^{207}Pb^*/^{206}Pb^*$	% err	$^{207}Pb^*/^{235}U$	% err	$^{206}Pb^*/^{238}U$	% err	err corr	$^{206}Pb/^{238}U$	±
Sample RB-01 – Andesite of Del Salto Formation																
RB01-1	0.142	497	245	0.49	17.4	24.5	0.8	0.0509	1.5	0.286	1.7	0.041	0.8	0.45	257	2
RB01-3	0.000	327	341	1.04	12.0	23.5	0.8	0.0519	2.0	0.305	2.1	0.043	0.8	0.38	269	2
RB01-4	−0.176	293	175	0.60	10.5	24.0	0.9	0.0522	2.2	0.300	2.4	0.042	0.9	0.37	264	2
RB01-10	−0.509	154	85	0.55	5.6	23.6	1.0	0.0527	2.7	0.308	2.7	0.042	1.0	0.38	268	3
Sample RB-02 – Rhyolite of Marechemill Formation																
RB02-01	−0.165	130	254	1.95	3.9	28.4	0.9	0.0540	3.3	0.262	3.4	0.035	0.9	0.26	223	2
RB02-04	0.187	347	1097	3.16	11.3	26.4	0.5	0.0495	2.8	0.258	2.8	0.038	0.5	0.18	239	1
RB02-05	0.377	574	1133	1.97	18.3	26.9	0.5	0.0487	2.6	0.249	2.6	0.037	0.5	0.18	235	1
RB02-07	0.438	289	739	2.55	9.0	27.6	0.6	0.0490	3.0	0.244	3.1	0.036	0.6	0.18	229	1
RB02-09	0.286	464	1277	2.75	14.6	27.4	0.5	0.0508	2.2	0.256	2.2	0.037	0.5	0.23	231	1
RB02-10	0.000	210	484	2.30	6.5	27.6	0.6	0.0507	2.6	0.254	2.6	0.036	0.6	0.23	230	1
RB02-08	−0.146	614	1769	2.88	20.7	25.5	0.5	0.0519	1.5	0.280	1.6	0.039	0.5	0.29	248	1
Sample RB-03 – Tuff of Corral de Piedra Formation																
RB03-01	−0.493	273	190	0.70	8.9	26.4	0.6	0.0510	2.2	0.288	2.1	0.038	0.6	0.29	240	2
RB03-02	−0.214	102	99	0.97	3.3	26.6	1.0	0.0535	3.6	0.286	5.4	0.038	1.0	0.18	238	2
RB03-03	−0.352	211	123	0.58	6.8	26.4	0.6	0.0494	2.7	0.273	3.4	0.038	0.6	0.19	239	2
Sample RB-04 – Tuff of Marechemill Formation																
RB04-01	−0.277	304	381	1.250	10.4	25.1	0.6	0.0524	2.0	0.288	2.1	0.040	0.6	0.28	251	2
RB04-02	−0.102	196	185	0.947	6.7	25.0	0.7	0.0514	2.7	0.283	2.8	0.040	0.7	0.26	253	2
RB04-04	0.699	207	93	0.451	36.5	4.9	0.6	0.0816	2.1	2.305	2.2	0.205	0.6	0.29	1201	8
RB04-05	−0.047	168	57	0.338	26.1	5.5	0.7	0.0712	1.2	1.772	1.4	0.181	0.7	0.49	1070	7
RB04-06	−0.258	58	92	1.595	10.3	4.8	1.3	0.0809	1.6	2.308	2.1	0.207	1.3	0.61	1212	15
RB04-07	−0.164	679	388	0.571	26.1	22.3	0.4	0.0531	1.2	0.328	1.3	0.045	0.4	0.29	282	1
RB04-08	0.411	52	53	1.012	9.9	4.5	1.3	0.0841	2.5	2.565	2.8	0.221	1.3	0.45	1289	16
RB04-09	0.495	103	104	1.011	9.1	9.8	0.9	0.0576	3.5	0.812	3.6	0.102	0.9	0.26	628	6
RB04-10	−0.135	523	362	0.693	20.6	21.8	0.5	0.0525	1.4	0.332	1.5	0.046	0.5	0.31	289	1
RB04-11	−0.200	326	137	0.422	12.9	21.7	0.5	0.0533	1.8	0.338	1.8	0.046	0.5	0.27	290	1
Sample RB-05 – Tuff of Corral de Piedra Formation																
RB05-02	0.42	230	339	1.47	7.73	25.5	1.6	0.0486	4.1	0.263	4.4	0.039	1.6	0.37	248	4
RB05-03	0.49	234	306	1.31	7.75	25.9	2.2	0.0503	4.6	0.268	5.1	0.039	2.2	0.43	244	5
RB05-04	1.09	120	138	1.15	4.23	24.4	1.9	0.0431	9.8	0.243	10.0	0.041	1.9	0.19	258	5
RB05-06	1.11	144	153	1.06	4.96	25.0	1.7	0.0428	8.2	0.236	8.4	0.040	1.7	0.21	253	4
RB05-07	0.14	262	436	1.66	9.12	24.7	1.6	0.0511	2.8	0.286	3.2	0.041	1.6	0.50	256	4
RB05-08	0.24	70	31	0.44	11.70	5.1	1.9	0.0734	2.6	1.976	3.2	0.195	1.9	0.59	1149	22
RB05-09	0.95	137	149	1.09	4.64	25.3	1.8	0.0419	11	0.228	10.7	0.039	1.8	0.17	250	5
RB05-10	0.69	153	259	1.70	4.97	26.4	1.7	0.0447	6.5	0.233	6.7	0.038	1.7	0.25	239	4
RB05-11	0.75	136	219	1.61	4.56	25.6	1.7	0.0464	4.0	0.250	4.3	0.039	1.7	0.39	247	4
Sample RB-06 – Rhyolite of Ciénega Redonda Formation																
RB06-01	−0.171	437	558	1.28	14.6	25.7	0.5	0.0521	1.6	0.280	1.7	0.039	0.5	0.29	246	1
RB06-03	0.000	195	168	0.86	6.7	25.2	0.7	0.0490	2.8	0.268	2.5	0.040	0.7	0.29	253	2
RB06-04	0.273	2010	1374	0.68	67.3	25.6	0.3	0.0496	1.8	0.267	1.8	0.039	0.3	0.17	247	1
RB06-05	0.228	344	201	0.58	11.5	25.7	0.5	0.0475	2.0	0.255	2.1	0.039	0.5	0.24	246	1
RB06-06	0.000	202	125	0.62	6.7	25.8	0.7	0.0523	2.5	0.280	2.5	0.039	0.7	0.28	246	2
RB06-07	0.000	496	300	0.60	16.2	26.3	0.5	0.0513	1.5	0.269	1.6	0.038	0.5	0.29	241	1
RB06-08	0.000	230	172	0.75	7.8	25.4	0.7	0.0498	2.3	0.270	2.3	0.040	0.7	0.28	250	2

Errors are 1-sigma; Pb_c and Pb^* indicate the common and radiogenic portions, respectively.
Error in Standard calibration was 0.57% (not included in above errors but required when comparing data from different mounts).
(2) Common Pb corrected by assuming $^{206}Pb/^{238}U$-$^{207}Pb/^{235}U$ age-concordance.

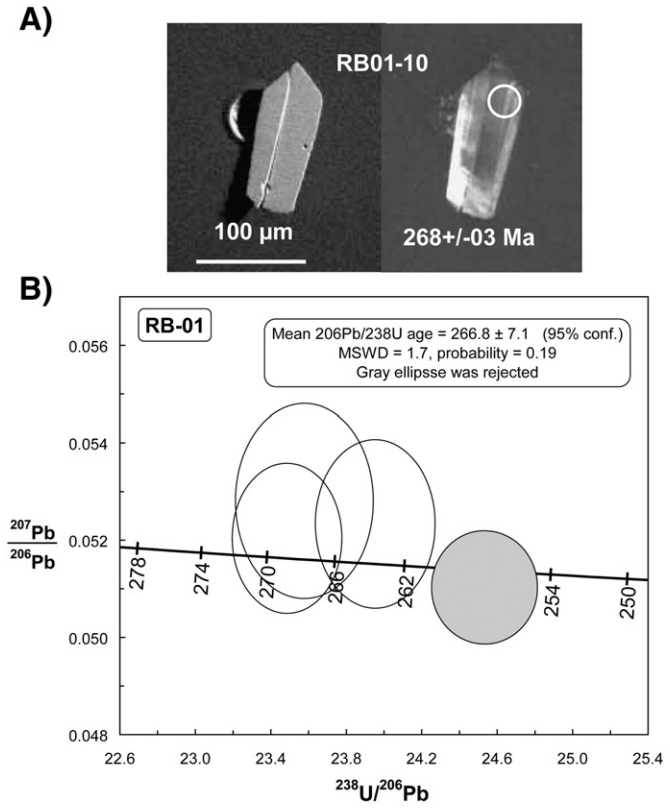

Fig. 5. A) BSE and CL images with spots and ages of the dated zircon from samples RB-01. B) U/Pb concordia ages obtained from the andesite of Del Salto Formation zircon sample RB-01 by SHRIMP spot analyses.

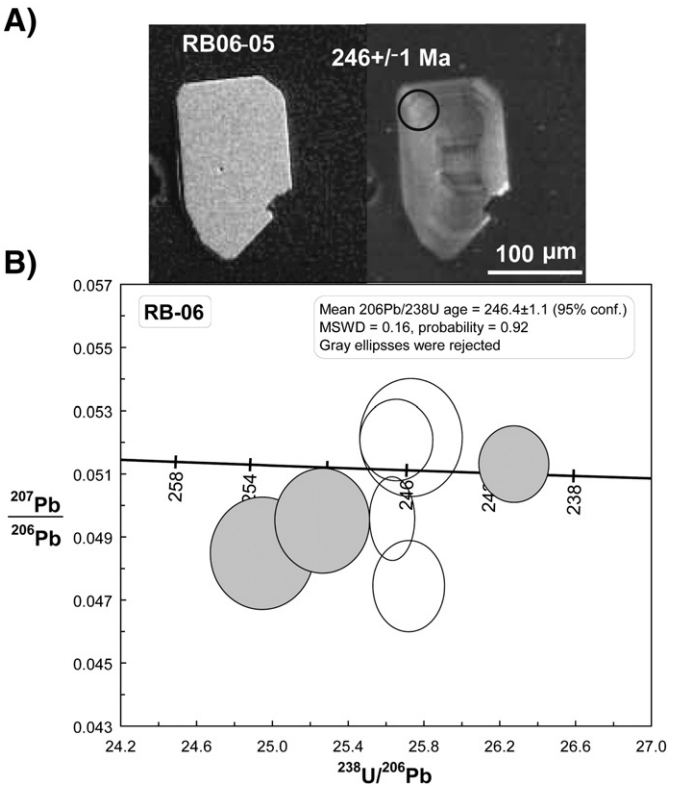

Fig. 6. A) BSE and CL images with spots and ages of the dated zircon from samples RB-01. B) U/Pb Concordia ages obtained from a rhyolite of Ciénaga Redonda Formation zircon sample RB-06 by SHRIMP spot analyses.

distinguished from those formations in spite of its apparently lateral stratigraphic continuity (Fig. 2). Marachemill sandstones also contain thinly laminated black shales clasts of the Carrizalito Formation which suggests that the Marachemill Unit is younger (Barredo and Ramos, 2010).

3. Analytical methods

After detailed mapping on a 1:15,000 scale of the Rincon Blanco sub-basin (Barredo, 2004), five volcanic and volcaniclastic samples of the Rincon Blanco sub-basin and one andesite sample of the underlying basement rocks were collected. Samples were crushed and milled using jaw crusher. Then, the zircons were separated by conventional procedures using heavy liquids and a sand magnetic separator after concentration by hand panning. The most clear and inclusion-free zircons from the least magnetic fractions were hand picked for U–Pb sensitive high resolution ion microprobe (SHRIMP) and laser ablation – multicollector – inductively coupled plasma mass spectrometry (LA-MC-ICPMS) analyses.

U–Pb SHRIMP zircon geochronology was carried out at the Research School of Earth Sciences, Australian National University and at the

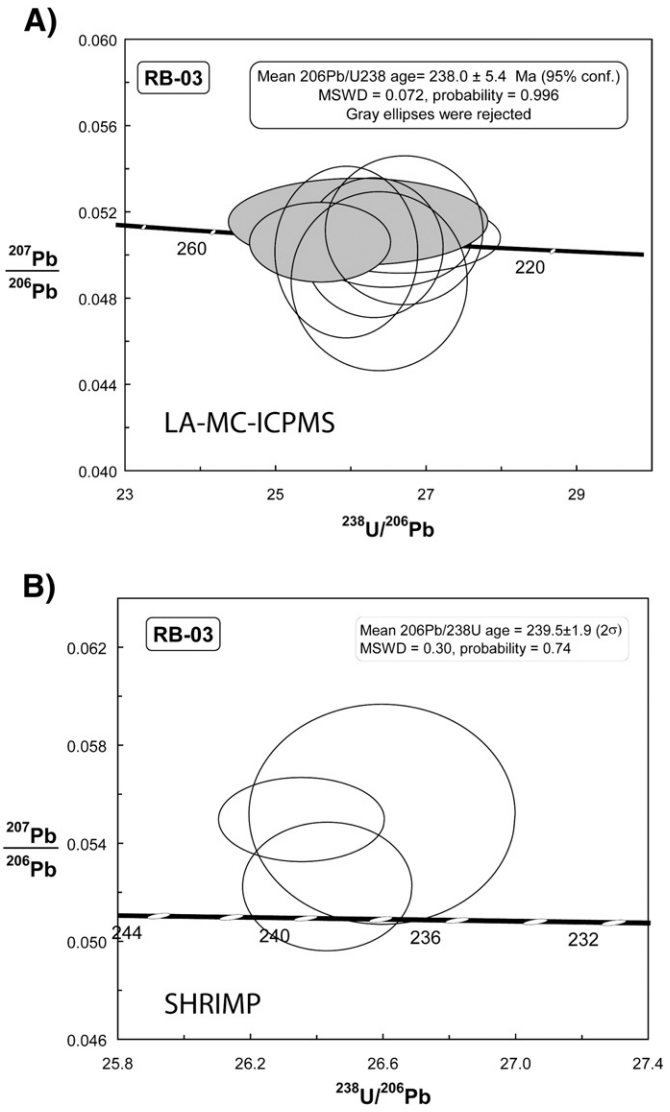

Fig. 7. U/Pb concordia ages obtained in a Corral de Piedra Formation tuff from zircon sample RB-3: A) LA-MC-ICPMS large spot analyses and B) by SHRIMP spot analyses (Chemale et al., 2008).

Department of Geology and Geophysics, University of Western Australia using SHRIMP II and RG equipments. Handpicked zircons were mounted in epoxy discs along with zircon standards, ground and polished, photographed in transmitted and reflected light, and imaged using scanning electron microscope (backscattered electrons – BSE). The mounts were then cleaned and gold-coated in preparation for SHRIMP analysis. Analytical methods and data treatment can be found elsewhere (Compston et al., 1984; Williams, 1998). Zircons grains were analyzed with a 2–3 nA, 10 kV primary O2- beam focused to a ~25 to ~20 μm diameter spot. At mass resolution ~5500 the Pb, Th and U isotopes were resolved from all other major interference isotopes. Reduction of raw data and age calculation were carried out using Squid 2.02 and Isoplot-Ex (Ludwig, 2003). U and Th concentrations were determined relative to those measured in the RSES standard SL13 and Temora.

For the laser ablation technique, all zircons were mounted in epoxy in 2.5-cm-diameter circular grain mounts and polished until the zircon interiors were just revealed. Images of zircons were obtained using an optical microscope (Leica MZ 125) and back-scatter electron microscope (Jeol JSM 5800). Zircon grains were dated with laser ablation system (New Wave UP213) coupled to a MC-ICP-MS (Thermo Scientific Neptune) at the Isotope Geology Laboratory of UFRGS (Universidade Federal do Rio Grande do Sul). Isotope data were acquired using static mode with spot size of 40 μm. Laser-induced elemental fractional and instrumental mass discrimination were corrected by the reference zircon (GJ-1) (Simon et al., 2004), following the measurement of two GJ-1 analyses to every ten sample zircon spots. The external error is calculated after propagation of the error of the GJ-1 mean and the individual sample zircon (or spot). Laser operating conditions are summarized in Table 1 and detailed description of analytical method can be found in Guadagnin et al. (2010).

The analytical data are presented in the Tables 1 and 2 as appendixes.

4. Results

The basal unit is exposed in northeast area of the Rincon Blanco sub-basin and it is represented by an andesite of the upper member of the Del Salto Formation. A sample was obtained from this andesite (RB-01: 31°17′18.53″ S–69°16′57.03″ W; see location in the inset of Fig. 2 and Fig. 3). Four SHRIMP spot analyses on four zircons were obtained, but the youngest one is discordant due to due to Pb loss, therefore not include in age calculation. Based on three data points, a 238U/206Pb age of 266.8 ± 7.1 (95% conf.) with MSWD of 1.7 was obtained (Fig. 5), which we have interpreted to represent the magmatic crystallization age of the andesite. These results make it possible to assign the entire Del Salto Formation to the early to middle Permian in in agreement with brachiopod fossils found in its lower section (Manceñido, 1973). The obtained age is similar to the K-Ar 272 ± 4 Ma age of the Alcaparrosa porphyry exposed a few km to the west of the Del Salto Formation (Sillitoe, 1988).

In order to constrain the depositional age of the different sequences of the Rincón Blanco sub-basin, we collected five samples, described here as follows:

A sample of rhyolite layer (RB-06: 31° 32′ 58.72″ S–69° 13′ 11.86″ W) was collected from the basal section of the Ciénaga Redonda Formation, located in the southern sector of the Río Blanco sub-basin (location in Fig. 2). Seven SHRIMP spot analyses on zircons were obtained, from which four juvenile magmatic zircons provided a weighted mean 238U/206Pb age of 246.4 ± 1.1 Ma (95% conf.) with a MSWD of 0.6 (Fig. 6).

From the three selected tuff layers, we obtained a precise age for the sample RB-03 (31° 26′ 53.42″ S–69° 16′ 14.11″ W) (Fig. 2) of the Corral de Piedra Formation, collected in the most central portion of the basin, with 206Pb/238U age of 239.5 ± 1.9 Ma (2σ) with a MSWD = 0.30, based on three SHRIMP spots (Fig. 7A). Additional U–Pb dating on same zircon population were carried out by the LA-MC-ICPMS technique that gave the 206Pb/238 U age of 238.0 ± 5.4 Ma based on the six most concordant zircons (MSWD = 0.072, 9 conf.) from eight dated grains (Fig. 7B).

In contrast, sample RB-05 (31° 29′ 41.71″ S–69° 14′ 58.06″ W) (Fig. 2), collected just above the flora and tetrapod footprint-rich layer of this unit, has a range of ages for eight zircons from 239 ± 4 Ma to 258 ± 26 Ma and one zircon with an age of 1149 ± 37 Ma. The zircons

Table 3
Summary of LA-MC-ICPMS U–Pb zircon data for Rincon Blanco Subbasin samples.

Sample RB-02 – Rhyolite of Marechemill Formation													
Spot number	f206	$^{232}Th/^{238}U$	$^{238}U/^{206}Pb$	% error	$^{207}Pb/^{206}Pb$	% err	$^{207}Pb/^{235}U$	% err	$^{206}Pb/^{238}U$	% err	err corr	$^{206}Pb/^{238}U$	error
RB02-03 *	0.0000	2.35	27.063	1.30	0.0516	1.22	0.2631	1.78	0.0370	1.30	0.73	234	3
RB02-09*	0.0000	2.17	26.693	2.04	0.0515	1.25	0.2658	2.40	0.0375	2.04	0.85	237	5
RB02-18*	0.0000	1.60	27.577	1.30	0.0514	1.14	0.2570	1.73	0.0363	1.30	0.75	230	3
RB02-20*	0.0000	2.52	26.965	1.32	0.0514	1.10	0.2628	1.72	0.0371	1.32	0.77	235	3
RB-02-21*	0.0000	1.70	27.603	1.31	1.8410	1.70	0.2594	1.84	0.0362	1.31	0.71	229	3
RB02-22*	0.0000	2.01	26.797	1.41	0.0528	1.09	0.2719	1.78	0.0373	1.41	0.79	236	3
RB02-34*	0.0000	2.44	27.317	1.27	0.0515	1.12	0.2600	1.69	0.0366	1.27	0.75	232	3
Sample RB-03 – Tuff of Corral Piedra Formation													
Spot number	f206	$^{232}Th/^{238}U$	$^{238}U/^{206}Pb$	% error	$^{207}Pb/^{206}Pb$	% err	$^{207}Pb/^{235}U$	% err	$^{206}Pb/^{238}U$	% err	err corr	$^{206}Pb/^{238}U$	error
RB03-16	0.0003	0.80	26.599	2.79	0.0511	2.91	0.265	4.03	0.038	2.79	0.69	238	7
RB03-16	0.0000	1.16	26.219	4.33	0.0519	2.57	0.273	5.04	0.038	4.33	0.86	241	10
RB03-21	0.0011	0.75	26.424	2.31	0.0507	4.24	0.265	4.83	0.038	2.31	0.48	239	6
RB03-11	0.0005	0.75	25.716	2.41	0.0509	2.40	0.273	3.40	0.039	2.41	0.71	246	6
RB03-12	0.0000	0.81	26.500	2.91	0.0491	5.60	0.256	6.31	0.038	2.91	0.46	239	7
RB03-07	0.0016	0.81	26.834	2.57	0.0515	4.44	0.265	5.13	0.037	2.57	0.50	236	6
RB03-10	0.0019	1.56	26.062	2.40	0.0505	5.21	0.267	5.73	0.038	2.40	0.42	243	6
RB03-03	0.0003	1.98	26.795	3.24	0.0511	2.12	0.263	3.87	0.037	3.24	0.84	236	8

1. Sample and standard are corrected after Pb and Hg blanks.
2. $^{207}Pb/^{206}Pb$ and $^{206}Pb/^{238}U$ are corrected after common Pb presence. Common Pb assuming $^{206}Pb/^{238}U$-$^{207}Pb/^{235}U$ concordant age.
3. $^{235}U = 1/137.88$*Utotal.
4. Standard GJ-1.
5. $Th/U = {}^{232}Th/^{238}U * 0.992743$.
6. All errors in the table are calculated 1 sigma (% for isotope ratios, absolute for ages).

crystallized from 258 to 1149 Ma are interpreted as xenocrysts. The youngest age of 239 ± 4 Ma can be related to syn-depositional volcanic contribution, similar to that dated in the sample RB-03 (Table 3).

Sample RB-02 (31°23′78″S–69°15′58.64″ W, location in Fig. 2), is a second rhyolite sample interlayered in sediments of the Marachemill Unit, which does not contain fossil. Three of seven SHRIMP spot analyses yielded an age of 230.3 ± 1.5 Ma, since the four other dated zircons were discordant (Fig. 8A). We also carried out zircon analyses by the LA-MC-ICPMS method . The three most concordant zircons yielded a 206Pb/238U age of 230.3 ± 3.4 Ma (Fig. 8B). Both ages point to a crystallization age of the Marachemill Unit rhyolite of 230 Ma.

A tuff collected from the Marachemill Unit in the eastern portion of the basin (RB-04: 31°25′35.22″S–69°15′14.08″W) (Fig. 2) yields several age populations. Two zircons yield a 206Pb/238U age of 251 ± 2.4 Ma, three zircons yield a concordant 206Pb/238 U age of 289.5 ± 2 Ma, one zircon is concordant at 628 ± 6 Ma while four zircons ranging from 1070 ± 7 Ma to 1289 ± 16 Ma.

Based on the dated zircon ages obtained from the tuffs of the Corral de Piedra (RB-05) and Marachemill (RB-04), we were also able to recognize inherited zircons as indicative of different source areas for the basin itself which yielded ages from 250, 253, 258, 390 and 628 Ma and Grenvillian ones (from 1070 to 1289 Ma). The presence of the Grenvillian ages support the Grenvillian TDM ages (Nd model ages) obtained for sediments and volcanic rocks of the contemporaneous Cacheuta sub-basin as presented by Avila et al. (2006) and from several other places in the Andes at these latitudes (Ramos, 2010).

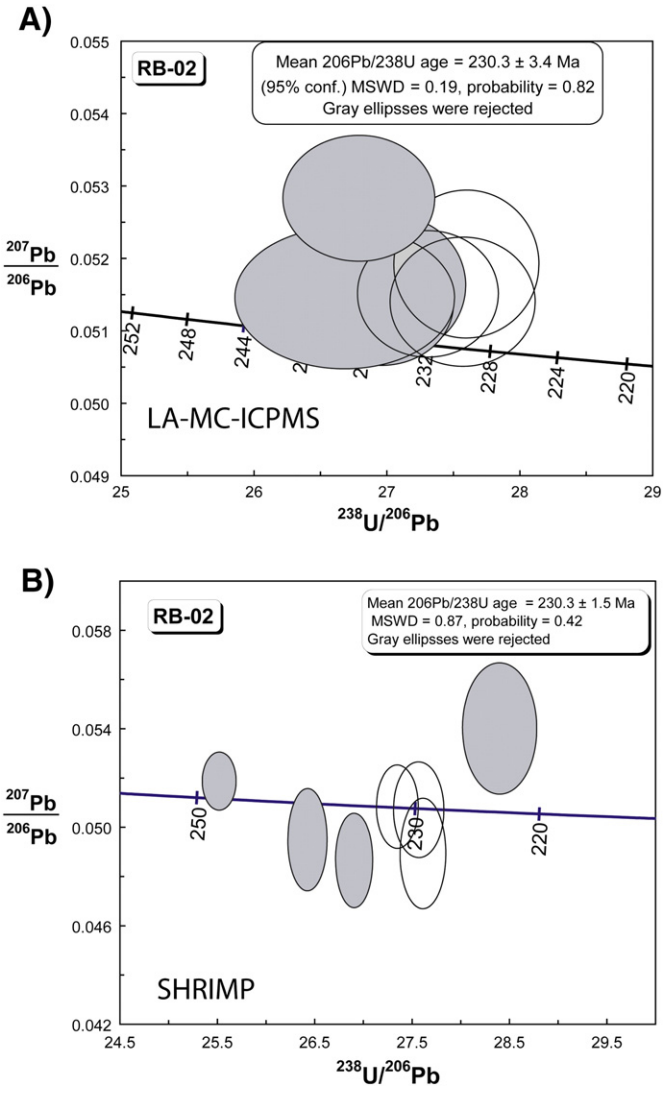

Fig. 8. U/Pb concordia ages obtained in a Marechemill Formation rhyolite from zircon sample RB-2: A) by SHRIMP spot analyses and B) by LA-MC-ICPMS large spot analyses.

5. Discussion

The infill of the Cuyo Basin can be divided in three tectono-sequences separated by erosional and low angle unconformities, all of them associated with extensional pulses. The first depositional sequences of the Cuyo Basin (Puntudo, Rincon Blanco and Cacheuta depocenters) are coeval with the latest Choiyoi tholeiitic magmatism, thus suggesting that the Cisuralian magmatic arc was still active. The younger sequences of Choiyoi rocks are crustal melts which formed together with basaltic underplating when subduction ceased (Kay et al., 1989). Using the temporal framework discussed herein, the first rifting pulse (synrift I), characterized by alluvial- fluvial and shallow lacustrine deposits, can be correlated along the different sub-basins. U–Pb zircon dating from the Cacheuta and Puntudo sub-basins (Avila et al., 2006; Mancuso et al., 2010) and data presented herein for the Rincón Blanco depocenter (246 ± 1.1 Ma yielded by the ignimbrite interlayered in the Ciénaga Redonda Formation) constrained this first tectono-sequence to the base of the Anisian (early Middle Triassic), according to the Triassic timescale of Furin et al. (2006).

A second significant reactivation of the faults gave place to the development of a regional unconformity that can be correlated across the depocenters. It has been interpreted as being an intra-Triassic tectonic event, probably associated with an extensional pulse in the west margin (Llambías et al., 2007). This second tectono-stratigraphic package (synrift II) represents a complete rift cycle with initial, climax, and post-rift stages sensu Prosser (1993). It is characterized by alluvial–fluvial and extended lake deposits which also mark a change from a semiarid to a more humid climate conditions when compared with the underlying sequence. The absolute dates obtained for the Rincón Blanco depocenter (Corral de Piedra Formation) yield an age of 239.5 ± 1.9 Ma which overlaps with a recent U–Pb zircon date of 239.2 ± 4.5 Ma for the Potrerillos Formation (Cacheuta sub-basin) (Spalletti et al., 2008). These dates constrain the deposition of the second sequence in the Cuyo rift to the base of the Ladinian (upper Middle Triassic, Furin et al., 2006).

The last extensional event recorded is not regionally found. At present, best exposures associated with this event are only found in the Rincón Blanco Sub-basin (Barredo and Ramos, 2010). The significant north displacement of the Marachemill Unit maximum thickness suggests the presence of another fault segment, which interacted with the ancient border structure, which finally became inactive (Barredo and Ramos, 2010). The syn-tectonic sedimentation related to this depocenter migration was included in the synrift III by Barredo and Ramos (2010). This third stage of rifting has been observed in the active margin as well as in the hanging-wall outcrops, and in the subsurface (Zamora-Valcarce et al., 2008). The infill is represented by an alluvial–fluvial succession developed under renewed mechanical subsidence of the basin and marked semiarid conditions. The present study has provided a U–Pb zircon age of 230.3 ± 1.5 Ma (SHRIMP) suggesting an early Carnian age for its deposition (lower Late Triassic, Furin et al., 2006).Therefore, the evolution of the basin can be constrained to the Middle-early Late Triassic (Fig. 9).

Extensional events along the western margin of Gondwana record three main pulses. During the Permo-Triassic, extension related to the breakup of Gondwana was expressed as rifting and graben formation along the Panthalassan margin (Veevers et al., 1994). In western Argentina, extensional relaxation, after the climax of Guadalupian–Early–Early Triassic volcanism, led to rapidly subsiding, fault-bounded, narrow troughs related to extension in the retroarc, as the Bermejo, Marayes, and Cuyo basins, among others (Uliana et al., 1988; Ramos and Kay, 1991). According to the results discussed herein, the Cuyo Basin, associated with this second extensional pulse, occurred

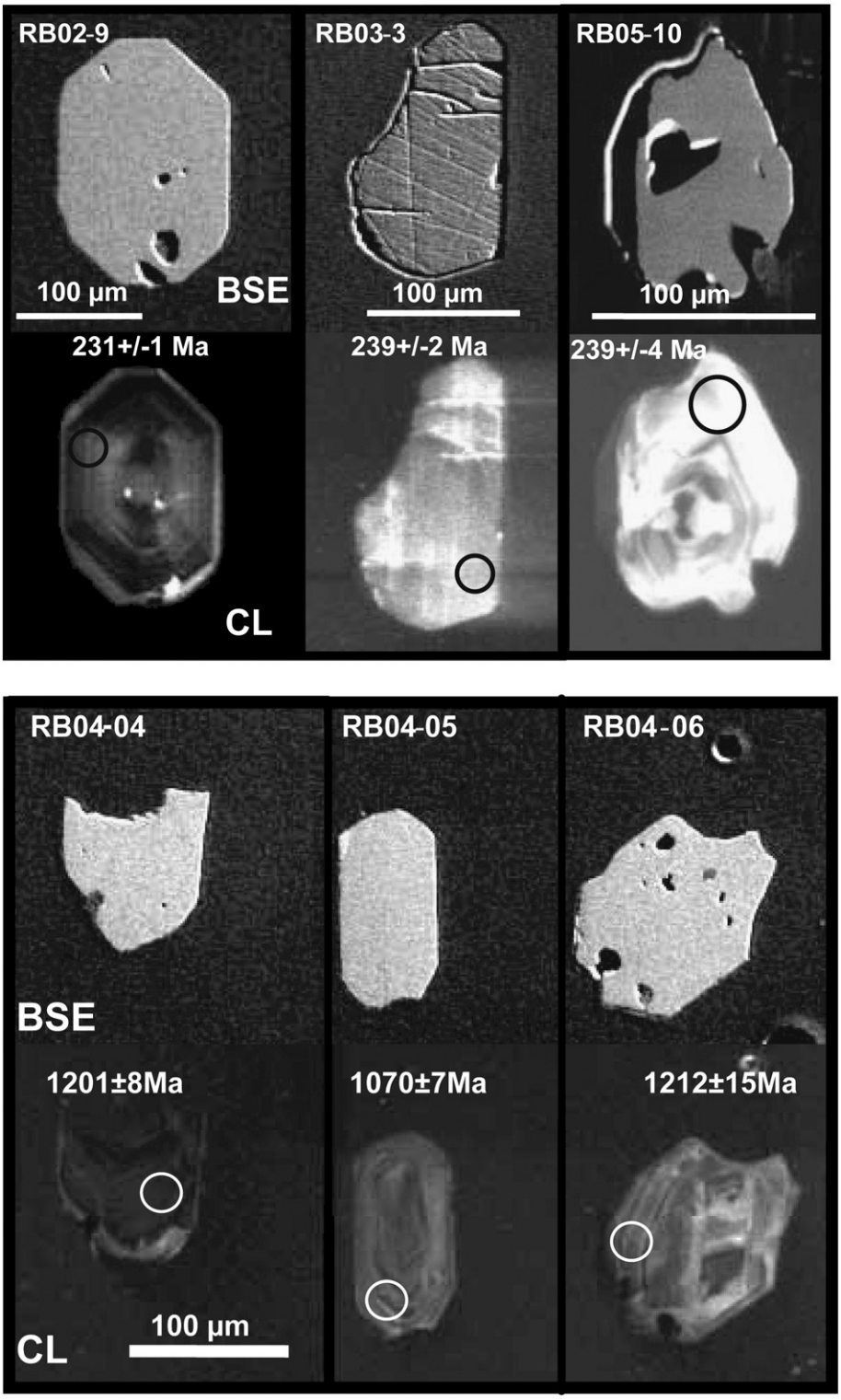

Fig. 9. BSE and Cl images with spots and ages of the dated zircons from samples RB-2 (Marechemill Rhyolite), RB-3 (Corral de Piedra Tuff) and inherited zircons of tuffaceous material of the Marechemill Unit (RB-04).

mainly during the Middle Triassic. The third extensional local event (Late Triassic-Early Jurassic) is coeval with the opening of the Neuquén Basin located farther south in northern Patagonia (Llambías et al., 2007). Regionally, it is also possible to recognize a north-south propagation of the extensional regime, which follows lithospheric weaknesses related to the Gondwanan orogen (e.g. Ramos, 2009; Barredo and Stinco, 2010). Accordingly, the Bermejo Basin opened first with its infill spanning the Early-Late Triassic (e.g. Milana and Alcober, 1994) followed by the Cuyo Basin, developed during the Middle Triassic (data presented herein). Southward in northern Patagonia, the Neuquén Basin was opened during the Late Triassic and evolved during the whole Mesozoic (e.g. Llambías et al., 2007). These Triassic rifting events have been also recognized along the cratonic areas in southern Brazil by Hackspacher et al. (2004) and Zerfass et al. (2005), and in different sectors of

Gondwana along previous collision sutures (Sorkhabi and Stump, 2001; Lakshminarayana, 2002; Dilek et al., 2007; Boger, 2011).

Finally the present study poses doubts about the widely used correlations among the Cuyo sub-basins and other western Gondwanan Triassic basins based on biostratigraphy (both palynostratigraphy and plants). According to the data discussed, at present evidences of sedimentation during most of the Late Triassic (Norian and Rhaetian) is absent in the basin.

Acknowledgments

Field research was supported by UBACYT X182: 2008–2010 (V. A. R.) and PIP CONICET 5120 (E.G.O.). Additional financial support was provided by the Consejo Nacional de Investigaciones Científicas y Técnicas (CONICET) and Conselho Nacional de Desenvolvimento Científico e Tecnológico (CNPq). This is contribution R-28 to the Instituto de Estudios Andinos Don Pablo Groeber (IDEAN).

References

Avila, J.M., Chemale Jr., F., Kawashita, K., Armstrong, R., Cingolani, C.A., 2003. Sm-Nd isotopic signature and U–Pb SHRIMP zircon dating of the Cacheuta Sub-basin, Cuyo Basin, NW Argentina. 4° South American Symposium on Isotope Geology (Salvador da Bahia), pp. 147–150 (Short Papers).

Avila, J.N., Chemale, F., Mallmann, G., Kawashita, K., Armstrong, R., 2006. Combined stratigraphic an isotopic studies of Triassic strata, Cuyo Basin, Argentine Precordillera. Geologial Society of America, Bulletin 118, 1088–1098.

Barredo, S.P., 2004. Análisis estructural y tectosedimentario de la subcuenca de Rincón Blanco, Precordillera Occidental, provincia de San Juan. PhD Thesis, Universidad de Buenos Aires (unpublished), 325 pp.

Barredo, S.P., 2005. Implicancias estratigráficas de la evolución de las fallas normales del hemigraben Rincón Blanco, cierre norte de la cuenca Cuyana, provincia de San Juan. 6° Congreso de Exploración y Desarrollo de Hidrocarburos, Actas electrónicas. 9 pp. Mar del Plata.

Barredo, S.P., Ramos, V.A., 2010. Características tectónicas y tectosedimentarias del hemigraben Rincón Blanco: una síntesis. Revista de la Asociación Geológica Argentina 66 (1–2), 133–145.

Barredo, S.P., Stinco, L., 2010. Geodinamica de las cuencas sedimentarias: su importancia en la localizacion de sistemas petroleros en Argentina. Revista Petrotecnia 2, 48–68.

Barredo, S.P., Stipanicic, P., 2002. In: Stipanicic, P.N., Marsicano, C.A. (Eds.), El Grupo Rincón Blanco: Léxico Estratigráfico de la Argentina, Asociación Geológica Argentina Serie B, 26, pp. 113–114.

Barredo, S.P., Ottone, G., Marsicano, C., Rodriguez Amenábar, C., 1999. Continental Biotic Association of the Triassic Rincón Blanco Subasin, Argentina. 7° International Symposium on Mesozoic Terrestrial Ecosystems (Buenos Aires), Actas, pp. 8–9.

Boger, S.D., 2011. Antarctica – before and after Gondwana. Gondwana Research 19, 335–371.

Borrello, A.V., Cuerda, A.J., 1965. Grupo Rincón Blanco (Triásico San Juan). Comisión de Investigaciones Científicas. Provincia Buenos Aires, Notas 2 (10), 3–20 (La Plata).

Brito Neves, B.B. de, Van Schmus, W.R., Fetter, A., 2002. North-western Africa-Northeastern Brazil. Major tectonic links and correlation problems. Journal of African Earth Sciences 34 (3–4), 275–278.

Chemale Jr., F., Kawashita, K., Dussin, I.A., Nunes, J.A., Justino, D., 2008. Age comparison between U–Pb zircon dating with LA-MC-ICP-MS using mixed detector configuration and SHRIMP. 6° South American Symposium on Isotope Geology. 2 pp. Bariloche.

Compston, W., Williams, I.S., Meyer, C., 1984. U–Pb geochronology of zircons from lunar breccia 73217 using a sensitive high-resolution ion-microprobe. Journal Geophysical Research B 98, 525–534.

Dilek, Y., Furnes, H., Shallo, M., 2007. Suprasubduction zone ophiolite formation along the periphery of Mesozoic Gondwana.

Furin, S., Preto, N., Rigo, M., Roghi, G., Gianolla, P., Crowley, J., Bowring, S., 2006. High-precision U–Pb zircon age from the Triassic of Italy: implications for the Triassic time scale and the Carnian origin of calcareous nannoplankton and dinosurs. Geology 34 (12), 1009–1012.

Gregori, D.A., Kostadinoff, J., Strazzere, L., Raniolo, A., 2008. Tectonic significance and consequences of the Gondwanide orogeny in northern Patagonia, Argentina. Gondwana Research 14 (3), 429–450.

Guadagnin, F., Chemale Jr., F., Dussin, I.A., Jelinek, A.R., dos Santos, Marcelo, N., Borba, M.L., Justino, D., Bertotti, A.L., Alessandretti, L., 2010. Depositional age and provenance of the Itajaí Basin, Santa Catarina State, Brazil: implications for SW Gondwana correlation. Precambrian Research 180, 156–182.

Hackspacher, P.C., Ribeiro, L.F.B., Ribeiro, M.C.S., Fetter, A.H., Hadler Neto, J.C., Tello, C.E.S., Dantas, E.L., 2004. Consolidation and Break-up of the South American Platform in Southeastern Brazil: Tectonothermal and Denudation Histories. Gondwana Research 7 (1), 91–101.

Kay, S.M., Ramos, V.A., Mpodozis, C., Sruoga, P., 1989. Late Paleozoic to Jurassic silicic magmatism at the Gondwanaland margin: analogy to the Middle Proterozoic in North America? Geology 17 (4), 324–328.

Kokogian, D.A., Seveso, F.F., Mosquera, A., 1993. Las secuencias sedimentarias triásicas. In: Ramos, V.A. (Ed.), Geología y Recursos Naturales de Mendoza. 12° Congreso Geología Argentina and 2° Congreso de Exploración de Hidrocarburos, Relatorio, pp. 65–78. Mendoza.

Kokogian, D.A., Spalletti, L.A., Morel, E.M., Artabe, A.E., Martínez, R.N., Alcober, O.A., Milana, J.P., Zavattieri, A.M., 2001. Estratigrafía del Triásico argentino. In: Artabe, A.E., Morel, E.M., Zamuner, A.B. (Eds.), El Sistema Triásico en la Argentina., Fundación Museo de La Plata Francisco Pascasio Moreno, pp. 23–54. La Plata.

Lakshminarayana, G., 2002. Evolution in basin fill style during the Mesozoic Gondwana continental break-up in the Godavari triple junction, SE India. Gondwana Research 5 (1), 227–244.

Legarreta, L., Kokogian, D.A., Dellape, D.A., 1992. Estructuración terciaria de la cuenca Cuyana: ¿Cuánto de inversión tectónica? Revista Asociación Geología Argentina 47 (1), 83–86.

Llambías, E.J., Leanza, H.A., Carbone, O., 2007. Tectono-magmatic evolution during the Permian to the Early Jurassic in the Cordillera del Viento (37°05′S-37°15′S): New Geological and Geochemical evidences for the early stages of the Neuquén basin. Revista de la Asociación Geológica Argentina 62 (2), 217–235.

López Gamundí, O.R., 1994. Facies distribution in an asymmetric half-graben: the northern Cuyo basin (Triassic), western Argentina. 14th International Sedimentological Congress, Abstracts, pp. 6–7. Recife.

Ludwig, K.R., 2003. User's Manual for Isoplot/Ex version 3.00 – a Geochronology Toolkit for Microsoft Excel, No. 4. Berkeley Geochronological Center Special Publication. 70 pp.

Manceñido, M.O., 1973. La fauna de la Formación Del Salto (Paleozoico superior de la Provincia de San Juan). Parte I: Introducción y estratigrafía. Ameghiniana 10 (3), 235–253.

Mancuso, A.C., Chemale, F., Barredo, S.P., Ávila, J., Ottone, E.G., Marsicano, C., 2010. Age constraints for the northernmost outcrops of the Triassic Cuyana Basin, Argentina. Journal of South American Earth Sciences 30 (2), 97–103.

Marsicano, C., Barredo, S.P., 2004. A Late Triassic tetrapod footprint assemblage from southern South America and its palaeoenviromental and palaeogeographical implications. Paleogeography, Paleoclimatology and Paleoecology 203, 313–335.

Milana, J.P., Alcober, O., 1994. Modelo tectosedimentario de la cuenca triasica de Ischigualasto (San Juan, Argentina). Revista de la Asociación Geológica Argentina 49, 217–235.

Mpodozis, C., Ramos, V.A., 2008. Tectónica jurásica en Argentina y Chile: extensión, subducción oblicua, rifting, deriva y colisiones? Revista de la Asociación Geológica Argentina 63 (4), 481–497.

Ottone, E.G., 2006. Plantas triásicas del Grupo Rincón Blanco, provincia de San Juan, Argentina. Ameghiniana 43, 477–486.

Ottone, E.G., Rodríguez Amenábar, C., 2001. A new disaccate pollen grain from the Triassic of Argentina. Ameghiniana 38, 157–161.

Prosser, S., 1993. Rift-related linked depositional systems and their seismic expression. In: Williams, G.D. and Dobb, A. (Eds.), Tectonic and sequence stratigraphy. Geological Society, Special Publication 71, 35–66. London.

Ramos, V.A., 2008. Patagonia: A Paleozoic continent adrift? Journal of South American Earth Sciences 26 (3), 235–251.

Ramos, V.A., 2009. Anatomy and global context of the Andes: main geologic features and the Andean orogenic cycle. In: Kay, S.M., Ramos, V.A., Dickinson, W. (Eds.), Backbone of the Americas: shallow subduction, plateau uplift, and ridge and terrane collision: Geological Society of América, Memoir, 204, pp. 31–65.

Ramos, V.A., 2010. The Grenville-age basement of the Andes. Journal of South American Earth Sciences 29 (1), 77–91.

Ramos, V.A., Kay, S.M., 1991. Triassic rifting and associated basalts in the Cuyo basin, central Argentina. In: Harmon, R.S., Rapela, C.W. (Eds.), Andean Magmatism and its Tectonic Setting: Geological Society of America, Special Paper, 265, pp. 79–91.

Rodríguez Amenábar, C., Ottone, E.G., 2003. La aplicación de Botryococcus (Chlorococcales) como indicador paleoambiental en el Triásico de Argentina. Revista Española de Micropaleontología 35, 25–35.

Sillitoe, R.H., 1988. Epochs of intrusion-related copper mineralization in the Andes. Journal of South American Earth Sciences, v. 1 (1), 89–108.

Simon, E., Jackson, S.E., Pearsona, N.J., Griffina, W.L., Belousova, E.A., 2004. The application of laser ablation-inductively coupled plasma-mass spectrometry to in situ U–Pb zircon geochronology. Chemical Geology 211, 47–69.

Sorkhabi, R., Stump, E., 2001. Intracontinental Rifting Along the Transantarctic Mountains in the Light of Gondwanaland Break-up and Tethyan Geodynamics. Gondwana Research 4 (4), 786–787.

Spalletti, L.A., 1999. Cuencas triásicas del Oeste Argentino: origen y evolución. Acta Geológica Hispánica 32 (1–2), 29–50.

Spalletti, L., Artabe, A., Morel, E., Brea, M., 1999. Paleofloristic biozonation and chronostratigraphy of the Argentine Triassic. Ameghiniana 36 (4), 419–451.

Spalletti, L.A., Fanning, C.N., Rapela, C.W., 2008. Dating the Triassic continental rift in the southern Andes, the Potrerillos Formation, Cuyo Basin, Argentina. Geologica Acta 6 (3), 267–283.

Stipanicic, P.N., 1972. Cuenca triásica de Barreal. In: Leanza, A.F. (Ed.), Geología Regional Argentina, Academia Nacional de Ciencias de Córdoba, pp. 537–566. Córdoba.

Stipanicic, P.N., 1979. El Triásico del Valle del río Los Patos (Provincia de San Juan). Segundo Simposio de Geología Regional Argentina, Academia Nacional de Ciencias, 2, pp. 695–744. Córdoba.

Stipanicic, P.N., 2002. Triásico. In: Stipanicic, P.N., Marsicano, C.A. (Eds.), Léxico Estratigráfico de la Argentina, 3. 870 pp., Buenos Aires.

Strelkov, E.E., Alvarez, L.A., 1984. Análisis estratigráfico y evolutivo de la cuenca triásica mendocina - sanjuanina. 9° Congreso Geología Argentina, Actas 3, 115–130.

Uliana, M.A., Biddle, K.T., Cerdan, 1989. Mesozoic–Cenozoic paleogeographic and geodynamic evolution of southern South America. Revista Brasileira de Geociencias 18, 172–190.

Veevers, J.J., 2005. Edge tectonics (trench rollback, terrane export) of Gondwanaland-Pangea synchronized by supercontinental heat. Gondwana Research 8 (4), 449–456.

Veevers, J.J., Cole, D.I., Cowan, E.J., 1994. Southern Africa: Karoo Basin and Cape Fold Belt. In: Veevers, J.J. y McA. Powell, C. (eds.) Permian-Triassic Pangean basins and foldbelts along the Panthalassan margin of Gondwanaland. Geological Society of America. Memoir 184, 223–279.

Williams, I.S., 1998. U–Th–Pb geochronology by ion microprobe. In McKibben, M.A., Shanks III, and W.C., Rydley, W.I. (eds.), Applications of Microanalytical Techniques to Understanding Mineralizing Processes. Revew Economic Geology 7, 1–35.

Yrigoyen, M.R., Stover, L.W., 1969. La palinología como elemento de correlación del Triásico en la cuenca Cuyana. 4° Jornadas Geológicas Argentinas, Actas 2, 427–447 Buenos Aires.

Zamora-Valcarce, G., Cervera, M., Barredo, S., 2008. Geología y potencial Petrolero de un bolsón intermontano: Bloque Tamberías, Provincia de San Juan. In: Schiuma, C. (Ed.), Trabajos Técnicos, 7° Congreso de Exploración y Desarrollo de Hidrocarburos, pp. 397–407. Mar del Plata.

Zavattieri, A.M., Batten, D.J., 1996. Miospores from Argentinian Triassic deposits and their potential for intercontinental correlation. In: Jansonius, J., McGregor, D.C. (Eds.), Palynology: principles and applications: American Association of Stratigraphic Palynologists Foundation, 2, pp. 767–778.

Zerfass, H., Chemale Jr., F., Lavina, E., 2005. Tectonic control of the Triassic Santa Maria supersequence of the Paraná Basin, southernmost Brazil, and its correlation to the Waterberg Basin, Namibia. Gondwana Research 8 (2), 163–176.